

# Rod Outer Segment Retinol Formation Is Independent of Abca4, Arrestin, Rhodopsin Kinase, and Rhodopsin Palmitylation

Lorie R. Blakeley,<sup>1</sup> Chunbe Chen,<sup>1</sup> Ching-Kang Chen,<sup>2</sup> Jeannie Chen,<sup>3</sup> Rosalie K. Crouch,<sup>1</sup> Gabriel H. Travis,<sup>4</sup> and Yiannis Koutalos<sup>1</sup>

**PURPOSE.** The reactive aldehyde all-*trans* retinal is released in rod photoreceptor outer segments by photoactivated rhodopsin and is eliminated through reduction to all-*trans* retinol. This study was undertaken to determine whether all-*trans* retinol formation depends on Abca4, arrestin, rhodopsin kinase, and the palmitylation of rhodopsin, all of which are factors that affect the release and sequestration of all-*trans* retinal.

**METHODS.** Experiments were performed in isolated retinas and single living rods derived from 129/sv wild-type mice and Abca4-, arrestin-, and rhodopsin kinase-deficient mice and in genetically modified mice containing unpalmitylated rhodopsin. Formation of all-*trans* retinol was measured by imaging its fluorescence and by HPLC of retina extracts. The release of all-*trans* retinal from photoactivated rhodopsin was measured in purified rod outer segment membranes according to the increase in tryptophan fluorescence. All experiments were performed at 37°C.

**RESULTS.** The kinetics of all-*trans* retinol formation in the different types of genetically modified mice are in reasonable agreement with those in wild-type animals. The kinetics of all-*trans* retinol formation in 129/sv mice are similar to those in C57BL/6, although the latter are known to regenerate rhodopsin much more slowly. The release of all-*trans* retinal from rhodopsin in purified membranes is significantly faster than the formation of all-*trans* retinol in intact cells and is independent of the presence of the palmitate groups.

**CONCLUSIONS.** The regeneration of rhodopsin and the recycling of its chromophore are not strongly coupled. Neither the

activities of Abca4, rhodopsin kinase, and arrestin, nor the palmitylation of rhodopsin affects the formation of all-*trans* retinol. (*Invest Ophthalmol Vis Sci.* 2011;52:3483–3491) DOI: 10.1167/iovs.10-6694

Rhodopsin, the primary light detector of vertebrate rod photoreceptor cells, is composed of a chromophore, 11-*cis* retinal, which is covalently bound to the apoprotein opsin.<sup>1,2</sup> Photon absorption isomerizes the chromophore to all-*trans*, leading to the generation of an active intermediate, metarhodopsin II, that initiates a cascade of reactions culminating in a change in membrane potential and hence the conversion of light to an electrical signal.<sup>3,4</sup> The cell recovery from light stimulation includes the deactivation of metarhodopsin II and of the other intermediates of the reaction cascade; metarhodopsin II is deactivated through its phosphorylation by rhodopsin kinase followed by the binding of arrestin. Necessary for recovery is also the regeneration of rhodopsin that was destroyed by the photoisomerization of its chromophore moiety. The regeneration is achieved through the removal of the all-*trans* chromophore and the binding of opsin with fresh 11-*cis* retinal, which is accomplished through a series of reactions called the visual cycle.<sup>5–7</sup>

The removal of the all-*trans* chromophore encompasses several steps, beginning with the hydrolysis of the Schiff base bond linking it to opsin, followed by its release from photoactivated rhodopsin as all-*trans* retinal. The all-*trans* retinal is subsequently reduced to all-*trans* retinol by retinol dehydrogenase,<sup>8,9</sup> and transferred from the rod outer segment to the adjacent retinal pigment epithelial cells by interphotoreceptor retinoid binding protein (IRBP).<sup>10,11</sup> In the retinal pigment epithelium, all-*trans* retinol is converted to 11-*cis* retinal,<sup>12</sup> which can then be used for the regeneration of rhodopsin.

The formation of all-*trans* retinol achieves the removal of the all-*trans* retinal released from the photoactivated rhodopsin. all-*trans* Retinal can form potentially toxic bisretinoid adducts with components of the rod outer segment<sup>13</sup> and is also a photosensitizer.<sup>14,15</sup> Because all-*trans* retinal is toxic and is also the substrate for the visual cycle, its processing in the rod outer segment has attracted considerable experimental attention. It has been shown that the binding of arrestin to photoactivated phosphorylated rhodopsin slows down the release of all-*trans* retinal.<sup>16,17</sup> After the release, all-*trans* retinal can remain noncovalently bound to opsin, to a site formed partly by the two palmitate groups attached to the opsin cysteines 322 and 323.<sup>18</sup> The all-*trans* retinal can also be sequestered inside the discs, bound via a Schiff base to phosphatidylethanolamine, and remain inaccessible to retinol dehydrogenase. The Abca4 transporter protein, present at the rim of the discs, is proposed to transport the phosphatidylethanolamine-all-*trans* retinal complex to the cytosolic side thereby making all-*trans* retinal available for reduction.<sup>19–21</sup> Defects in

From the <sup>1</sup>Department of Ophthalmology, Medical University of South Carolina (MUSC), Charleston, South Carolina; the <sup>2</sup>Department of Biochemistry and Molecular Biology, Virginia Commonwealth University, Richmond, Virginia; the <sup>3</sup>Zilkha Neurogenetic Institute, University of Southern California Keck School of Medicine, Los Angeles, California; and the <sup>4</sup>Jules Stein Eye Institute, University of California at Los Angeles School of Medicine, Los Angeles, California.

Supported by National Institutes of Health/National Eye Institute (NIH/NEI) Grants EY14850 (YK), EY13811 (CKC), EY12155 (JC), EY04939 (RKC), and EY011713 (GHT) and an unrestricted grant to MUSC Storm Eye Institute from Research to Prevent Blindness, Inc., New York, NY. RKC is a RPB Senior Scientific Investigator. Mice were housed in a facility constructed with support from NIH grant C06 RR015455 from the Extramural Research Facilities Program of the National Center for Research Resources.

Submitted for publication October 7, 2010; revised January 4 and February 24, 2011; accepted February 25, 2011.

Disclosure: L.R. Blakeley, None; C. Chen, None; C.-K. Chen, None; J. Chen, None; R.K. Crouch, None; G. H. Travis, None; Y. Koutalos, None

Corresponding author: Yiannis Koutalos, Department of Ophthalmology, Medical University of South Carolina, 167 Ashley Avenue, Charleston, SC 29425; koutalo@musc.edu.

the proteins involved in these reactions could result in increased levels of all-*trans* retinal consequent to light detection, restrict the amounts of available 11-*cis* retinal, or both. Importantly, such defects have been linked to serious visual deficiencies: Mutations in *Abca4* are responsible for Stargardt disease, a form of childhood macular degeneration,<sup>22,23</sup> and mutations in arrestin and rhodopsin kinase lead to Oguchi disease, a form of congenital stationary night blindness.<sup>24,25</sup>

To probe the relevance of these different factors in the clearance of all-*trans* retinal through its reduction to all-*trans* retinol, we measured the kinetics of all-*trans* retinol formation in the outer segments of rod photoreceptors separated from the pigment epithelium. In such a preparation, the all-*trans* retinol formed after exposure to light cannot be transported away and accumulates in the outer segment membranes. This process allows the examination of the steps involving all-*trans* retinal and resulting in all-*trans* retinol formation. We used retinas from wild-type and four types of genetically modified mice, lacking rhodopsin kinase (*Rbok*<sup>-/-</sup>), arrestin (*Sag*<sup>-/-</sup>), the *Abca4* transporter (*Abca4*<sup>-/-</sup>), or the palmitate groups of rhodopsin (*Palm*<sup>-/-</sup>). That is, they have biochemical defects that can influence either the release of all-*trans* retinal from photoactivated rhodopsin or its access to retinol dehydrogenase. We measured the formation of all-*trans* retinol by quantitative HPLC of retinoid extracts and from its fluorescence. For comparison, we separately measured the release of all-*trans* retinal from photoactivated rhodopsin in purified rod outer segment membranes. We found no substantial differences in the kinetics and levels of all-*trans* retinol formation between wild-type and the four types of genetically modified mice. The formation of all-*trans* retinol, however, is much slower than the release of all-*trans* retinal. It should be emphasized that the conclusions in this article are based solely on the data obtained from isolated retina and cell preparations and not from an intact eye.

In the rest of the text, retinal and retinol refer to the all-*trans* isomers.

## METHODS

Wild-type mice (129/sv) were from Harlan Laboratories (Indianapolis, IN). Genetically modified mice were from established colonies at the Medical University of South Carolina. *Rbok*<sup>-/-</sup> mice lack rhodopsin kinase,<sup>26</sup> *Sag*<sup>-/-</sup> lack arrestin,<sup>27</sup> and *Abca4*<sup>-/-</sup> the *Abca4* transporter,<sup>19</sup> and *Palm*<sup>-/-</sup> express a mutant rhodopsin that lacks the palmitate groups.<sup>28</sup> All animal procedures were performed in accordance with protocols approved by the Institutional Animal Care and Use Committee of the Medical University of South Carolina; the authors adhered to the ARVO Statement for the Use of Animals in Ophthalmic and Vision Research. The animals were kept in a cyclic 12-h light cycle (0600–1800 hours). For experiments, we used 2- to 3-month-old animals that were dark-adapted overnight and killed under dim red light. The retinas were excised under either dim red or infrared light in mammalian Ringer's (in mM: 130 NaCl, 5 KCl, 0.5 MgCl<sub>2</sub>, 2 CaCl<sub>2</sub>, 25 hemisodium-HEPES, 5 glucose [pH 7.40]). All reagents were of analytical grade.

HPLC measurements of retinoid extracts were conducted according to previously published procedures.<sup>29</sup> Briefly, isolated retinas were incubated at 37°C in bicarbonate Ringer's (in mM: 94 NaCl, 5 KCl, 0.5 MgCl<sub>2</sub>, 2 CaCl<sub>2</sub>, 25 hemisodium-HEPES, 24 NaHCO<sub>3</sub>, 5 glucose [pH 7.40]) gassed with 95% O<sub>2</sub> and 5% CO<sub>2</sub> (at 1 atm). Retinoids were extracted at different times after the retina was bleached with long-wavelength light (1 minute; >530 nm from a 150-W halogen lamp illuminator). Chromatography was performed with a commercial system (Waters Corp., Milford, MA) with a 250 × 4.6-mm, 5-μm column (LiChrospher Silica-60; Alltech Associates, Inc., Deerfield, IL) and a mobile phase made of hexanes (HPLC grade), ethyl acetate, dioxane, and octanol (85.4:11.2:2.0:1.4). The relative amount of a retinoid in the

sample was calculated from the area under its peak and its extinction coefficient, and the fraction of all-*trans* retinol was calculated from the relative amounts. In this way, measurement of the kinetics of retinol formation is not affected by the different number of rod outer segments present in individual preparations. One retina was used for each experimental determination and at least three determinations per time point.

Retinol fluorescence measurements were performed with retina slices and isolated rod photoreceptor cells, as described previously.<sup>29</sup> Briefly, fluorescence imaging experiments were performed on the stage of an inverted microscope (Axiovert 100; Carl Zeiss Meditec, Thornwood, NY), using 360 nm excitation and >420 nm emission. For slices, the objective was a water-immersion lens (40× Achroplan, NA = 0.8; Carl Zeiss Meditec), and for isolated cells an oil-immersion lens (40× Plan Neofluar, NA = 1.3; Carl Zeiss Meditec). The experiments were performed at 37°C, and to maintain the higher temperature, the microscope stage and the oil-immersion objective were heated (Warner Instruments, Hamden, CT). Fluorescence images were acquired at different times after bleaching a slice or an isolated cell with long-wavelength light (1 minute; >530 nm from a 150-W halogen lamp illuminator). Fluorescence intensity was measured over defined regions of interest (ROIs) in the outer segments and background. In experiments with slices, after correction for background, the fluorescence intensities were divided by the initial value before bleaching. In experiments with isolated cells, after correction for background, the initial value before bleaching was subtracted from all subsequent values to obtain the fluorescence due to retinol; retinol fluorescence was then converted to retinol concentration (in millimolar) through a calibration procedure using hexane/chloroform droplets containing a known concentration of all-*trans* retinol.

Rod outer segment membranes were purified from isolated wild-type and *Palm*<sup>-/-</sup> retinas as described elsewhere.<sup>30</sup> The final pellet was washed twice and finally suspended in a buffer containing (in mM) 100 KCl, 1 MgCl<sub>2</sub>, 1 CaCl<sub>2</sub>, 10 HEPES (pH 7.30) and used for the experiments. In one experimental approach, membranes were suspended at a rhodopsin concentration of 0.5 μM, and the kinetics of all-*trans* retinal release from bleached rhodopsin were determined from the increase in Trp fluorescence.<sup>31</sup> Trp fluorescence measurements were performed in a spectrofluorometer (Olis; Quantum Northwest, Inc., Liberty Lake, WA) with 295 nm excitation and collecting emission from 310 to 350 nm. The maximum amplitude of the Trp fluorescence trace was normalized to 1.0. In another approach, the kinetics of all-*trans* retinal release from bleached rhodopsin were measured from the amounts of regenerated rhodopsin after addition of a 5- to 10-fold excess of 11-*cis* retinal.<sup>32</sup> For all-*trans* retinal release measurements, rhodopsin was bleached in exactly the same way as for all-*trans* retinol formation measurements—that is, with 1 minute of long-wavelength light (>530 nm) from a 150-W halogen lamp illuminator. The maximum amplitude of the data, defined as the average value reached after 30 minutes, was normalized to 1.0. The experiments were performed at 37°C.

We used previously published approaches for analyzing the data and comparing the results from different techniques and mouse types.<sup>29</sup> We approximated retinol kinetics with two separate first-order processes, one for formation and one for elimination, with the rate constants  $f_1$  and  $f_2$ , respectively. For the measurements with whole retinas and retina slices, there is virtually no elimination of retinol and  $f_2 \approx 0$ . In that case, retinol accumulates in the tissue, its concentration  $C(t)$  increases with rate constant  $f_1$  and reaches a plateau rod outer segment concentration,  $C_0$ .

$$C(t) = C_0 \cdot (1 - e^{-f_1 \cdot t}) \quad (1a)$$

Because virtually all retinal had been released from the photoactivated rhodopsin (see Fig. 4) before the retinol concentration reached the plateau, retinal and retinol were at equilibrium at the plateau. This equilibrium was reached after sufficient NADPH had been generated to

convert a large fraction of the released retinal to retinol. The HPLC of retinoid extracts from whole retinas measured the kinetics of retinol formation from the retinol fraction, ROL(retina fraction), of the total all-*trans* chromophore. If  $P_0$  is the concentration of rhodopsin in the rod outer segment ( $P_0 \approx 3$  mM), then the total all-*trans* chromophore concentration (retinal plus retinol) after bleaching is also  $P_0$ , and

$$C(t) = \text{ROL}(\text{retina fraction}) \cdot P_0 \tag{1b}$$

The concentration of retinol at the plateau,  $C_0$  is given by  $C_0 = \beta \cdot P_0$ , where  $\beta$  is the fraction of retinol at long times after bleaching and at equilibrium with retinal. From equations 1a and 1b, the fraction ROL-(retina fraction) of all-*trans* chromophore converted to retinol at time  $t$  after bleaching is given by

$$\text{ROL}(\text{retina fraction}) = \beta \cdot (1 - e^{-f_1 \cdot t}) \tag{1'}$$

The fluorescence imaging of retina slices measures the kinetics of retinol formation from its fluorescence  $F(t)$ , which is proportional to its rod outer segment concentration  $C(t)$ . In the absence of removal, retinol accumulates, and its fluorescence reaches a plateau,  $F_{\text{max}}$ , corresponding to the concentration  $C_0$ .

$$F(t) = F_{\text{max}} \cdot (1 - e^{-f_1 \cdot t}) \tag{2a}$$

Because the fluorescence of the slice, ROL(slice fluorescence), is normalized by the basal fluorescence of the tissue before bleaching (this basal fluorescence is not due to retinol), we have

$$\text{ROL}(\text{slice fluorescence}) = 1 + F(t) \tag{2b}$$

and from equations 2a and 2b,

$$\text{ROL}(\text{slice fluorescence}) = 1 + F_{\text{max}} \cdot (1 - e^{-f_1 \cdot t}) \tag{2'}$$

In the case of isolated rod photoreceptors, the larger surface-to-volume ratio of the single cell allows for a substantial rate of retinol elimination—that is,  $f_2 > 0$ . In that case, the rod outer segment concentration of retinol  $C(t) = \text{ROL}(\text{cell})$  is given by

$$\text{ROL}(\text{cell}) = \frac{f_1 \cdot C_0}{f_1 - f_2} \cdot (e^{-f_2 \cdot t} - e^{-f_1 \cdot t}) \tag{3}$$

For  $f_2 = 0$ , equation 3 becomes equation 1a. It should be kept in mind that it is not necessarily the case that the parameters  $C_0$  and  $f_1$  in equation 3 have the same values as their counterparts in equation 1a. It is possible, for example, that the rate constant for retinol formation depends on its removal. We have found that this is not the case, however, and that the values of  $C_0$  and  $f_1$  determined from isolated cells are in agreement with those determined from whole retinas.

The kinetics of all-*trans* retinal release were described as the sum of two first-order processes, where  $A_1$  and  $A_2 = 1 - A_1$  are the relative amplitudes, and  $k_1$  and  $k_2$  are the rate constants (the maximum amplitudes of the data are normalized to 1.0). The fraction RAL of retinal that has been released at time  $t$  after rhodopsin bleaching is given by

$$\text{RAL} = 1 - A_1 \cdot e^{-k_1 \cdot t} - A_2 \cdot e^{-k_2 \cdot t} \tag{4}$$

Parameters were determined by least-squares fits (Kaleidagraph; Synergy, Reading PA). Errors for parameters were obtained from the curve fits.

## RESULTS

We have previously measured the kinetics of retinol formation in rod photoreceptors from wild-type C57BL/6 mice.<sup>29</sup> In the pres-

ent work, our purpose was to examine the kinetics of retinol formation in the rod photoreceptors of mice with deficiencies in factors implicated in the processing of retinal. To measure the kinetics of retinol formation, we used the same three experimental preparations as for the C57BL/6 mice (Fig. 1): whole retina (Fig. 1A), retina slice (Fig. 1B), and single isolated rod photoreceptors (Fig. 1C). Figure 1A shows the chromatographic profiles of retinoids extracted from whole retinas of mice lacking arrestin (*Sag*<sup>-/-</sup>), incubated for different times after bleaching. On light exposure, the 11-*cis* retinal chromophore (trace a) is isomerized to all-*trans* (trace b). Subsequently, all-*trans* retinal is converted to all-*trans* retinol and accumulates in the retina, and its fraction in the retinoid extract increases with time (traces c and d). From such chromatograms, we obtain the fraction of retinol as a function of time after bleaching. The kinetics of retinol formation can also be measured by imaging its fluorescence in retina slices and in isolated rod photoreceptors. Figure 1B shows the retinol fluorescence increase in the outer segment layer of a retina slice from a mouse lacking rhodopsin kinase

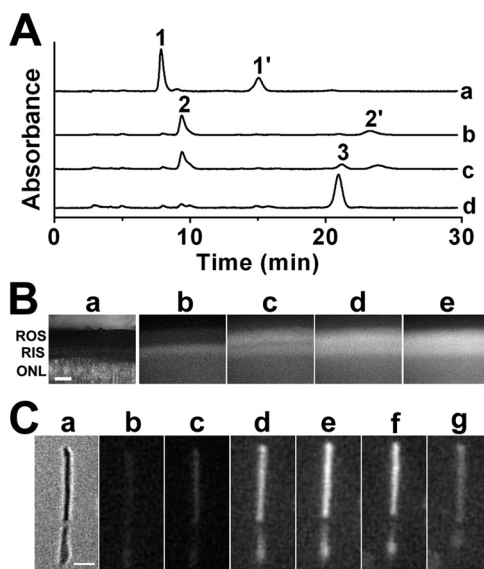


**FIGURE 1.** Three different methods for measuring the kinetics of all-*trans* retinol formation. (A) Quantitative HPLC of retinoid extracts. Chromatograms (at 325 nm) of retinoid extractions from isolated retinas of mice lacking arrestin (*Sag*<sup>-/-</sup>) and incubated for different times after bleaching at 37°C: (a) dark control; (b) immediately after bleaching; (c) 5 minutes; (d) 90 minutes after bleaching. 1, *syn*-11-*cis* retinal oxime; 1', *anti*-11-*cis* retinal oxime; 2, *syn*-all-*trans* retinal oxime; 2', *anti*-all-*trans* retinal oxime; 3, all-*trans* retinol. To allow comparisons, the traces have been normalized to the total amount of retinoid present in each sample. (B) Fluorescence imaging of retina slices. After the bleaching of rhodopsin, all-*trans* retinol fluorescence increased in the rod outer segment layer of a retina slice from a mouse lacking rhodopsin kinase (*Rbok*<sup>-/-</sup>): (a) infrared image of the photoreceptor layer of the unbleached retinal slice; ROS, rod outer segments; RIS, rod inner segments; ONL, outer nuclear layer; (b-e) fluorescence (excitation, 360 nm; emission, >420 nm) images of the photoreceptor layer; (b) before bleaching; (c) immediately after; (d) 10 minutes; (e) 90 minutes after bleaching. Images (b-e) are shown at the same scale. Experiment conducted at 37°C. Bar, 20  $\mu\text{m}$ . (C) Fluorescence imaging of single isolated rod photoreceptors. All-*trans* retinol fluorescence increased after rhodopsin bleaching in the outer segment of an isolated rod photoreceptor from a mouse lacking the *Abca4* transporter (*Abca4*<sup>-/-</sup>): (a) infrared image of the isolated rod photoreceptor; (b-g) fluorescence (excitation, 360 nm; emission, >420 nm) images of the cell; (b) before bleaching; (c) immediately after; (d) 10 minutes; (e) 30 minutes; (f) 60 minutes; (g) 90 minutes after bleaching. Images (b-g) are shown at the same scaling. Experiment conducted at 37°C. Bar, 5  $\mu\text{m}$ .

**TABLE 1.** Values of Parameters Describing the Kinetics of all-*trans* Retinol Formation, as Determined by Different Methods and for Tissues from Different Types of Mice

Mouse Type	Whole Retina		Retina Slice		Isolated Cell		
	$f_1$ (min <sup>-1</sup> )	$\beta$	$f_1$ (min <sup>-1</sup> )	$F_{\max}$	$f_1$ (min <sup>-1</sup> )	$f_2$ (min <sup>-1</sup> )	$C_0$ (mM)
C57BL/6	0.04 ± 0.01	0.82 ± 0.04	0.06 ± 0.01	6.1 ± 0.4	0.06 ± 0.02	0.024 ± 0.009	2.5 ± 0.7
129/sv	0.04 ± 0.01	0.74 ± 0.04	ND	ND	0.06 ± 0.01	0.024 ± 0.004	2.2 ± 0.2
Palm <sup>-/-</sup>	0.03 ± 0.01	0.85 ± 0.07	0.06 ± 0.01	5.3 ± 0.3	0.036 ± 0.003	0.024 ± 0.001	2.6 ± 0.2
Abca4 <sup>-/-</sup>	0.05 ± 0.01	0.72 ± 0.04	0.03 ± 0.01	7.6 ± 0.5	0.08 ± 0.01	0.016 ± 0.003	2.1 ± 0.2
Sag <sup>-/-</sup>	0.023 ± 0.003	0.90 ± 0.06	0.04 ± 0.01	7.2 ± 0.6	0.08 ± 0.02	0.012 ± 0.004	1.8 ± 0.3
Rbok <sup>-/-</sup>	0.030 ± 0.003	0.81 ± 0.03	0.03 ± 0.01	7.0 ± 0.6	0.07 ± 0.02	0.022 ± 0.006	2.4 ± 0.5

Parameters:  $f_1$ , rate constant for retinol formation (equations 1', 2', and 3);  $f_2$ , rate constant for retinol removal (equation 3);  $\beta$ , the fraction of the all-*trans* chromophore in the form of retinol at long times after bleaching and at equilibrium with retinal (equation 1');  $C_0$ , concentration of generated retinol (equations 1a, 3);  $F_{\max}$ , fold increase in basal rod outer segment layer fluorescence (equation 2'). ND, not determined.

(*Rbok*<sup>-/-</sup>); and Figure 1C shows the transient retinol fluorescence increase in the outer segment of an isolated rod photoreceptor from a mouse lacking the *Abca4* transporter (*Abca4*<sup>-/-</sup>). From such images, we obtain the fluorescence and concentration of retinol as a function of time after bleaching. The data from these three types of experiments were fitted with equations 1', 2', and 3, and the resultant values of the parameters describing the kinetics of retinol formation are given in Table 1.

### Kinetics of Retinol Formation in 129/sv Wild-Type Mice

Initially, we characterized retinol formation in rod photoreceptors from 129/sv wild-type mice, because, along with C57BL/6, they are the background of most genetically modified animal strains. In addition, because of an amino acid difference in the Rpe65 protein of the retinal pigment epithelium, the visual cycle operates much faster in 129/sv than in C57BL/6 mice.<sup>33,34</sup> Thus, it is important to test for possible additional differences between the strains. Figure 2 shows that the kinetics of retinol formation in the rod outer segments of 129/sv mice (circles) were similar to those of C57BL/6 (lines), with the values of the parameters determined by the fits being virtually the same (Table 1). Only the steady state level of the fraction of retinol,  $\beta$ , appeared to be somewhat lower in the 129/sv mice than in the C57BL/6 (Fig. 2A, Table 1), but this conclusion is not borne out by the similar values of the  $C_0$  parameter, which is proportional to  $\beta$ . In Figure 2B, the value of  $C_0$  (2.2–2.5 mM) for 129/sv and C57BL/6 rod cells (Table 1) is much larger than the peak value of the rod outer segment

retinol concentration (~1.4 mM). This difference is due to the significant elimination of retinol in the isolated cell, which does not allow its concentration to reach the level of  $C_0$ . Similarly, as shown in Figures 3C, 4C, and 5C, the peak values of the rod outer segment retinol concentration were much lower than the values for  $C_0$  (Table 1).  $C_0$  is the concentration retinol would reach in the absence of elimination.

### Kinetics of Retinol Formation in *Abca4*-Deficient Mice

The *Abca4* transporter has been proposed to facilitate the transfer of all-*trans* retinal from the disc lumen to the cytosolic disc surface, where it can be reduced to all-*trans* retinol by retinol dehydrogenase.<sup>19,35</sup> Lack of *Abca4* would be expected to limit the availability of all-*trans* retinal for reduction. The kinetics of retinol formation in mice lacking the *Abca4* transporter (*Abca4*<sup>-/-</sup>) are similar to those in wild type (Fig. 3), and the values of the kinetic parameters determined by the fits are in good agreement with those in wild type (Table 1). The slice data (Fig. 3B, squares) do not appear to be described well by the wild-type curve (solid line), but this likely reflects the impact of the simplified modeling of retinol formation with a single first-order process (see the Discussion section).

### Kinetics of Retinol Formation in Arrestin- and Rhodopsin Kinase-Deficient Mice

The binding of arrestin to phosphorylated photoactivated rhodopsin slows down the release of all-*trans* retinal.<sup>16,17</sup> Lack of arrestin binding, either because of arrestin deficiency or lack of rhodopsin phosphorylation would be expected to speed up the availability of all-*trans* retinal for reduction. The kinetics of retinol formation in mice lacking arrestin (*Sag*<sup>-/-</sup>) or rhodopsin kinase (*Rbok*<sup>-/-</sup>) are similar to those in the wild type (Figs. 4A–C). The values of the kinetic parameters determined by the fits are in good overall agreement with those in the wild type (Table 1). The deviations from the wild type in the slice data (Fig. 4B) probably reflect the impact of the simplified model (see also Fig. 3B). The retinol formation kinetics in *Sag*<sup>-/-</sup> retinas appear to be significantly slower than in wild type (Fig. 4A, Table 1), however, this is not borne out in the single-cell data (Fig. 4C, Table 1). Similar considerations apply for the discrepancy in the values of the  $C_0$  parameter between *Sag*<sup>-/-</sup> and wild-type mice (Table 1). Given the close agreement between the *Sag*<sup>-/-</sup> and wild-type single-cell data (Fig. 4C), it appears that the discrepancy may reflect the sensitivity of the model parameters to the specific data values. Such an interpretation is corroborated by the higher value of the steady state fraction of retinol as determined from whole retinas.

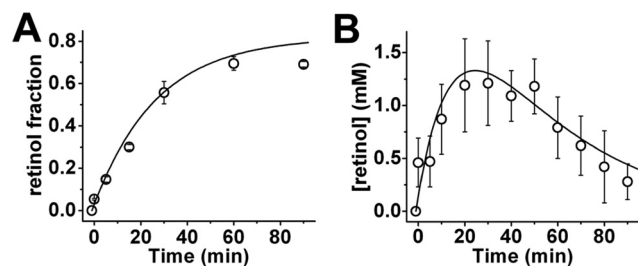
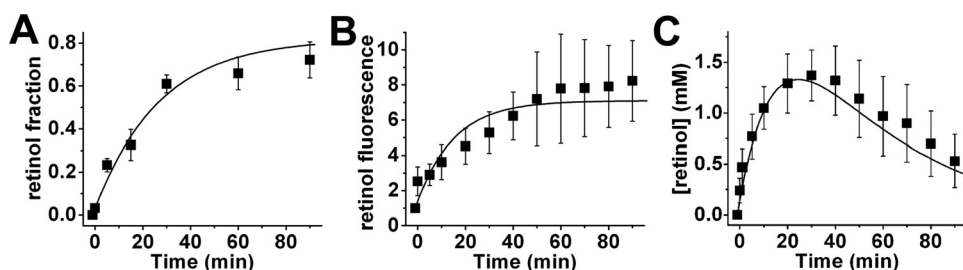


**FIGURE 2.** Similar kinetics of all-*trans* retinol formation after bleaching in 129/sv (○) and C57BL/6 mice (solid lines). (A) Fraction of retinol in retinas at different times after bleaching, measured with HPLC of extracted retinoids. (B) Retinol concentration in the outer segments of single isolated rod photoreceptors at different times after bleaching ( $n = 5$  cells from 129/sv). Solid lines: the best fits for the published data from C57BL/6 wild-type mice.<sup>29</sup> Bleaching was performed between  $t = -1$  minute and  $t = 0$ . Error bars, SD. All experiments were conducted at 37°C.

**FIGURE 3.** The kinetics of all-*trans* retinol formation after bleaching in the rod outer segments from *Abca4*<sup>-/-</sup> mice (■) were similar to those from C57BL/6 wild-type mice (solid lines). (A) Fraction of retinol in retinas at different times after bleaching, measured with HPLC of extracted retinoids. (B) Retinol fluorescence in the outer segment layer of slices at different times after bleaching (*n* = 9 slices from *Abca4*<sup>-/-</sup>). (C) Retinol concentration in the outer segments of single isolated rod photoreceptors at different times after bleaching (*n* = 8 cells from *Abca4*<sup>-/-</sup>). Solid lines: the best fits for the published data from C57BL/6 wild-type mice.<sup>29</sup> Bleaching was performed between *t* = -1 minute and *t* = 0. Error bars represent standard deviations. All experiments were conducted at 37°C.



*Rbok*<sup>-/-</sup> mice provide us with an opportunity to compare the kinetics of retinol formation with those of retinal release from photoactivated rhodopsin. Retinal release can be readily measured in purified rod outer segment membranes, where, as in living *Rbok*<sup>-/-</sup> cells, photoactivated rhodopsin is not phosphorylated, and there is no binding of arrestin. We measured retinal release after bleaching in purified mouse rod outer segment membranes in two ways: first, from the increase in opsin tryptophan fluorescence associated with retinal leaving the chromophore-binding pocket,<sup>31</sup> and, second, from the amount of rhodopsin regenerated on the addition of 11-*cis* retinal, which is equivalent to the concentration of empty chromophore-binding pockets.<sup>32</sup> The two methods give simi-

lar results for wild-type rhodopsin (Fig. 4D). These experiments with purified membranes were performed at a pH of 7.3 and at 37°C. The release kinetics involved more than one component and were described as the sum of two first order processes (equation 4). The amplitudes and rate constants for the two processes were obtained by fitting the data in Figure 4D with equation 4, and are given in Table 2. The release of retinal was faster than the formation of retinol. From the Trp fluorescence trace, we found that 90% of retinal had been released by 23 minutes, whereas, using the curve fit for the retinol data, we found that the retinol concentration reached 90% of its plateau in 56 minutes. This is a time lag of more than 30 minutes between retinal release and retinol formation.

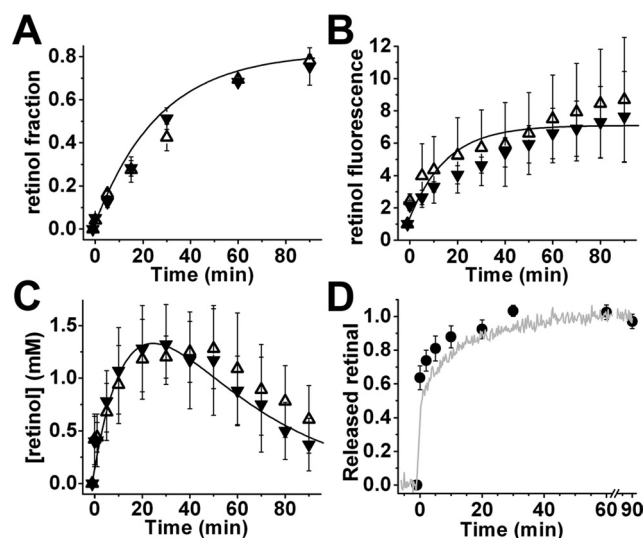


**FIGURE 4.** Kinetics of all-*trans* retinol formation in rod outer segments from *Sag*<sup>-/-</sup> and *Rbok*<sup>-/-</sup> mice compared with kinetics of all-*trans* retinal release from photoactivated rhodopsin. (A) Fraction of retinol in retinas (*Sag*<sup>-/-</sup>,  $\Delta$ ; *Rbok*<sup>-/-</sup>,  $\nabla$ ) at different times after bleaching, measured with HPLC of extracted retinoids. (B) Retinol fluorescence in the outer segment layer of slices at different times after bleaching (*Sag*<sup>-/-</sup>,  $\Delta$ , *n* = 8; *Rbok*<sup>-/-</sup>,  $\nabla$ , *n* = 9). (C) Retinol concentration in the outer segments of single isolated rod photoreceptors at different times after bleaching (*Sag*<sup>-/-</sup>,  $\Delta$ , *n* = 12; *Rbok*<sup>-/-</sup>,  $\nabla$ , *n* = 16). (A-C, solid lines) the best fits for the data from C57BL/6 wild-type mice.<sup>29</sup> (D) Kinetics of the release of all-*trans* retinal from bleached wild-type rhodopsin in rod outer segment membranes. All-*trans* retinal release was measured from the increase in Trp fluorescence (excitation: 295 nm; emission: 310 to 350 nm; gray line, average of six experiments) and from the amount of regenerated rhodopsin on addition of 11-*cis* retinal at different times after bleaching (●; at least four determinations per time point). The maximum amplitudes of the data are normalized to 1.0. All experiments were conducted at 37°C, with bleaching performed between *t* = -1 minute and *t* = 0. Error bars, SD.

### Kinetics of Retinol Formation in Mice Containing Unpalmitylated Rhodopsin

The palmitate groups of rhodopsin form a retinoid binding site that could sequester retinal after its release from the chromophore-binding pocket.<sup>18</sup> The kinetics of retinol formation in mice containing a mutant rhodopsin that lacks the palmitate groups (*Palm*<sup>-/-</sup>) were similar to those in the wild type (Figs. 5A-C), and the values of the kinetic parameters determined by the fits were in good overall agreement with those in the wild type (Table 1). As with the previous strains, the formation kinetics were biphasic (Figs. 5B, 5C), but they were described with a single kinetic parameter,  $f_1$ . As before, this is probably the reason for the slight deviations from wild type in the values of the parameters in Table 1.

The palmitate groups may contribute to the differences between rhodopsin and cone pigments that lack cysteines in the corresponding positions; photoactivated cone pigments release retinal much faster than rhodopsin Kuemmel CM, et al. *IOVS* 2008;49:ARVO E-Abstract 1664.<sup>36</sup> We found that the kinetics of retinal release from unpalmitylated rhodopsin in purified rod outer segment membranes were virtually identical with those from wild-type rhodopsin (Fig. 5D, Table 2).

**TABLE 2.** Values of Parameters Describing the Kinetics of all-*trans* Retinal Release from Wild-Type and Unpalmitylated Rhodopsins

	$A_1$	$k_1$ (min <sup>-1</sup> )	$k_2$ (min <sup>-1</sup> )
Wild-type Rh regeneration	0.65 ± 0.05	2.7 ± 1.1	0.10 ± 0.02
Wild-type Trp fluorescence	0.51 ± 0.01	1.3 ± 0.1	0.068 ± 0.002
Unpalmitylated Trp fluorescence	0.48 ± 0.01	3.9 ± 1.3	0.069 ± 0.001

Parameters:  $A_1$ , amplitude of the rapid component of retinal release (component with rate constant  $k_1$ ; equation 4);  $k_1$  and  $k_2$ , rate constants for retinal release (equation 4).

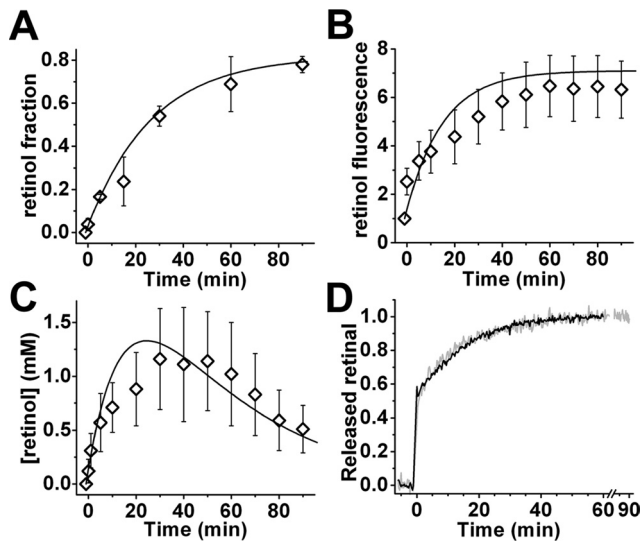


**FIGURE 5.** Kinetics of all-*trans* retinol formation in rod outer segments from *Palm*<sup>-/-</sup> ( $\diamond$ ) mice and kinetics of all-*trans* retinal release from photoactivated unpalmitylated rhodopsin. (A) Fraction of retinol in retinas of *Palm*<sup>-/-</sup> ( $\diamond$ ) mice at different times after bleaching, measured with HPLC of extracted retinoids. (B) Retinol fluorescence in the outer segment layer of *Palm*<sup>-/-</sup> slices ( $\diamond$ ,  $n = 6$ ) at different times after bleaching. (C) Retinol concentration in the outer segments of single isolated *Palm*<sup>-/-</sup> rod photoreceptors ( $\diamond$ ,  $n = 8$ ), at different times after bleaching. (A–C, *solid lines*), the *solid lines* represent the best fits for the corresponding data from C57BL/6 wild-type mice.<sup>29</sup> (D) Kinetics of the release of all-*trans* retinal from bleached unpalmitylated rhodopsin (measured from Trp fluorescence; *black line*, average of four determinations) in rod outer segment membranes. Plotted for comparison are the kinetics of release from wild-type (palmitylated) rhodopsin (*gray line*). The maximum amplitudes of the data are normalized to 1.0. All experiments (A–D) conducted at 37°C, with bleaching performed between  $t = -1$  minute and  $t = 0$ . Error bars, SD.

## DISCUSSION

A striking feature of our results is the lack of any substantial difference in retinol formation between wild-type mice and mice that lack important enzymes and rhodopsin modifications. It is important that the agreement holds across the different experimental preparations of whole retinas, retina slices, and single cells, making it unlikely that the results are affected by any physical trauma suffered during tissue isolation. This consistency is especially relevant for the results from *Sag*<sup>-/-</sup> and *Rbok*<sup>-/-</sup> mice, in which the health of the photoreceptor cells may be compromised as the retinas degenerate with age.<sup>27,37</sup> For each of the different strains, the value of the rate constant for retinol formation,  $f_1$ , is similar to that in the wild type,  $\sim 0.06$  minute<sup>-1</sup>. There appear to be statistically significant differences in the values of the parameters (Table 1) across the different mouse types, but this most likely reflects the sensitivity of the parameters to slight differences in data values, as there was overall close agreement between the experimental data across mouse types (Figs. 2–5). The systematically lower values for  $f_1$  as determined by HPLC of retinoids from whole retinas (Table 1) are probably due to the underestimation of the values of the retinol fraction at low retinol concentrations due to losses during extraction.<sup>32</sup> Although retinol formation is biphasic, composed of a rapid and a slow phase, we approximated the overall formation kinetics with a single rate constant. There may be slight differences between the strains, especially in the rapid phase of retinol formation, that are beyond the resolution of the present experiments.

An important difference in the formation of retinol in isolated cells or retina tissues compared with the situation in situ

is the absence of its vigorous removal by IRBP. It is possible that the rate constant for retinol formation was substantially increased by its removal by IRBP, and the different types of experiments presented here provide some relevant information. In retina tissue, retinol is not being eliminated, but in the isolated cell, it leaves the cell even in the absence of IRBP (hence, the substantial decrease in fluorescence beginning after approximately 30 minutes). As the data in Table 1 show, the rate constant for retinol formation (parameter  $f_1$ ) in the isolated cells (0.04–0.08 minute<sup>-1</sup>) is higher than in whole retinas (0.02–0.05 minute<sup>-1</sup>). As pointed out before, one contributing factor to this difference is the underestimation of the values of the retinol fraction at low retinol concentrations due to losses during extraction. Consistent with this interpretation, the  $f_1$  values measured with fluorescence from retina slices (0.03–0.06 minute<sup>-1</sup>) are higher than those measured with extraction from retinas (0.02–0.05 minute<sup>-1</sup>) and slightly lower than those measured from cells. The remaining discrepancy in the  $f_1$  values between retina slices and isolated cells may be due to experimental variability or to the elimination of retinol speeding up its formation in isolated cells. In the latter case, we would expect that in the intact eye, the presence of IRBP would speed up retinol formation compared with the isolated cells. Experiments to test such a contribution of IRBP on the rate of retinol formation are feasible, but require large amounts of purified IRBP. Such an effect of IRBP, however, may be small, in view of the good agreement between the rate constant for retinol formation of  $\sim 0.06$  minute<sup>-1</sup> reported here and the time constant of 15 minutes for the clearance of retinal after bleaching as determined in whole animals.<sup>38</sup> In addition, for frog rod photoreceptors, the rate constant for retinol formation is not affected by its removal either by 1% bovine serum albumin (see Fig. 4B in Ref. 32) or by physiological concentrations of IRBP (compare Figs. 4A and 4B in Ref. 32 taking into account the different Y-axis scales).

Apart from the same rate constant for retinol formation, different mouse strains also have the same fraction of total chromophore converted to retinol at equilibrium,  $\beta \approx 0.8$ , as measured from whole retinas. Since the mouse rod outer segment rhodopsin concentration is  $P_0 \approx 3$  mM,<sup>39</sup> this fraction corresponds to a retinol concentration at equilibrium of  $C_0 \approx 2.4$  mM, in good agreement with the determinations from isolated rods (Table 1). Because the fraction of retinol at equilibrium depends on the reduced fraction of NADPH, the result suggests that the reducing environment of the rods is the same in the different strains, and the lack of enzymes has not interfered with redox balance. The reduced fraction of NADPH corresponding to a retinol fraction of 0.8 is  $\sim 0.2$ ,<sup>32</sup> in good agreement with histochemical measurements.<sup>40</sup>

## Retinol Formation Kinetics Do Not Correlate with Rhodopsin Regeneration Kinetics

We find no substantial difference in the kinetics of rod outer segment retinol formation between 129/sv and C57BL/6 wild-type mice (Fig. 2, Table 1). This result confirms that the much slower rate of rhodopsin regeneration in C57BL/6 mice<sup>33,34</sup> is not related to the reactions occurring in the outer segment after rhodopsin bleaching (see the Discussion section in Ref. 29). It further shows that a slower regeneration of rhodopsin is not accompanied by any compensation in the processing of chromophore in the outer segment. This observation points to the recycling of the chromophore and the regeneration of rhodopsin as not being strongly coupled; they may be independent processes.

### Retinol Formation Is Unaffected by the Sequestration of Retinal

The rhodopsin palmitate groups are one factor that can affect the availability of all-*trans* retinal for reduction after its release from photoactivated rhodopsin. The palmitate groups form part of a retinoid binding site,<sup>18</sup> to which retinal could bind after its release, limiting its availability for reduction. Our results with the Palm<sup>-/-</sup> mice indicate, however, that retinol formation is not faster in the absence of the palmitate groups. This finding suggests that any sequestration of retinal by the palmitate retinoid binding site does not limit its reduction by retinol dehydrogenase.

Another factor that affects the availability of retinal for reduction is the *Abca4* transporter. Absence of a functional *Abca4* transporter results in the trapping of all-*trans* retinal in the disc lumen of the rod outer segment with no access to retinol dehydrogenase.<sup>19</sup> This phenomenon results in the accumulation of bis-retinoid adducts in the rod outer segments and the deposition of large amounts of lipofuscin (including bis-retinoids such as A2E) in the retinal pigment epithelium.<sup>19,41-43</sup> Large depositions of lipofuscin and bis-retinoids are also found in the retinal pigment epithelium of Stargardt patients.<sup>19</sup> The similarity in the kinetics of retinal clearance between wild-type and *Abca4*<sup>-/-</sup> mice found in the present experiments suggest that no more than a small fraction of retinal ends up depending on the *Abca4* transporter for access to retinol dehydrogenase. Such a small fraction of retinal could be below the detection limit of the experiments presented here, but over time could lead to the accumulation of significant levels of retinal adducts in the rod outer segment and bis-retinoids in the retinal pigment epithelium. The similarity in the kinetics of retinal clearance is also relevant for the recovery of sensitivity of the retina after exposure to bright light, a process referred to as dark adaptation. Retinal can activate opsin,<sup>44,45</sup> which would slow down the recovery of the rod photoreceptors from light excitation,<sup>46</sup> and may explain the originally reported delay in the dark adaptation of *Abca4*<sup>-/-</sup> mice.<sup>19</sup> No significant delay was found in subsequent experiments with mice, however.<sup>47</sup> The results reported here suggest that any differences in the kinetics of dark adaptation between wild-type and *Abca4*<sup>-/-</sup> mice do not originate in the rod photoreceptor cells.

### Retinol Formation Is Unaffected by the Acceleration of Retinal Release

Although the *Abca4* transporter and the rhodopsin palmitate groups might impact the availability of the released retinal for reduction, the binding of arrestin to phosphorylated photoactivated rhodopsin slows down the release of retinal.<sup>16,17</sup> Therefore, we expect that the release of retinal in rods lacking arrestin or rhodopsin kinase would be faster than in the wild type. It should be kept in mind that arrestin translocates out of the rod outer segment in the absence of light,<sup>48-51</sup> and so, in an acutely bleached dark-adapted rod outer segment, the concentration of arrestin present would be sufficient to slow down the release of retinal from only a fraction of the photoactivated rhodopsin.<sup>52</sup> Thus, we would expect the effects of rhodopsin kinase and arrestin to manifest themselves in the initial rapid increase of retinol after photoactivation. The measurements presented here did not show any discernible differences in the rapid phase or in the overall kinetics of retinol formation between rods from *Sag*<sup>-/-</sup>, *Rbok*<sup>-/-</sup> and wild-type mice. This finding suggests that retinal release does not limit retinol formation.

### Retinol Formation is Slower Than Retinal Release

The kinetics of retinal release from photoactivated rhodopsin in purified rod outer segment membranes were faster than the kinetics of retinol formation measured in metabolically intact rod outer segments from all mouse strains examined. In combination with retinol formation's being unaffected by the sequestration of retinal or by the speeding up of its release, this result points to the reduction reaction's being the step that determines the kinetics of retinol formation. Specifically, the data are consistent with NADPH availability being the limiting factor. Approximately half of the all-*trans* retinal chromophore of photoactivated rhodopsin was swiftly released (Figs. 4D, 5D), and a significant portion was readily reduced to retinol, as indicated by the substantial amplitude of the rapid component of retinol formation.<sup>29,53</sup> Subsequently, the cell appears to boost NADPH production to further promote the conversion of retinal to retinol. This process takes time, and as a result, the formation of retinol lags significantly behind the release of retinal.

We have described the kinetics of retinal release from photoactivated rhodopsin as the sum of two first-order processes (Table 2). There is a rapid component, the kinetics of which are not well-resolved in our measurements and which is consistent with the fast release of retinal from metarhodopsin II.<sup>54</sup> The slower component likely reflects the slow decay of metarhodopsin III.<sup>54,55</sup> 11-*cis* Retinal does not facilitate the release of all-*trans*, as indicated by the close agreement between the release kinetics measured from Trp fluorescence and from regeneration with added 11-*cis* retinal. The palmitate groups may contribute to the differences between rhodopsin and cone pigments that lack cysteines in the corresponding positions. In agreement with this role, Palm<sup>-/-</sup> rod photoreceptors recover faster from light excitation than do wild-type ones.<sup>28</sup> Retinal is released faster from cone pigments than is rhodopsin,<sup>36</sup> but the lack of the palmitate groups of rhodopsin did not affect the kinetics of retinal release (Fig. 5D, Table 2). This finding extends to physiological pH and temperature, with the previous result obtained in detergent at room temperature.<sup>56</sup>

Because of the considerable time lag of more than 30 minutes between retinal release and its reduction to retinol and the significant toxicity of retinal,<sup>57</sup> the health of the rod photoreceptor depends on containing free retinal. Metarhodopsin III provides a long-storage form of photoactivated rhodopsin that would slow down retinal release, as previously suggested.<sup>55</sup> Retinal release would be slowed down even further through the phosphorylation of photoactivated rhodopsin by rhodopsin kinase and arrestin binding. This mechanism is likely to be particularly relevant under continuous light conditions, when arrestin translocates to the rod outer segment and can bind to a large fraction of photoactivated rhodopsin.<sup>52</sup> On the other hand, absence of a functional rhodopsin kinase or arrestin would result in the build-up of all-*trans* retinal. This could be a factor in the light-dependent retina degeneration observed in *Rbok*<sup>-/-</sup><sup>26</sup> and *Sag*<sup>-/-</sup><sup>37</sup> mice, and in particular the degeneration that is independent of the activation of the phototransduction cascade.<sup>58</sup> Functional defects in arrestin and rhodopsin kinase have been found to be responsible for Oguchi disease, a form of night blindness. Although no significant retina degeneration has been observed in Oguchi patients, the potential build-up of all-*trans* retinal levels in rods reinforces the previous recommendation of avoiding exposure to bright light.<sup>37</sup>

After its release, retinal is eventually detoxified through its reduction to retinol. If it ends up inside the discs, the *Abca4* transporter facilitates its transfer to the cytosolic side, where it has access to retinol dehydrogenase. Consistent with the need to prevent accumulation of retinal inside the discs, lack of a

functional Abca4 transporter has been associated with retinal toxicity.<sup>57</sup> On the cytosolic side of the disc, the toxicity of retinal is checked through sequestration by the palmitate group binding site. Although there are no reports of human visual defects associated with lack of rhodopsin palmitylation, Palm<sup>-/-</sup> mice are more susceptible to light-induced damage than the wild type,<sup>59</sup> consistent with a protective role of the palmitate groups. It should be emphasized that the palmitate groups exert their protective role, not by preventing the accumulation of retinal, but rather through its sequestration.

A major factor in the clearance of retinal that was not addressed in the present work is the removal of retinol by IRBP, the carrier present in the interphotoreceptor space. IRBP would speed up the removal of retinol and, through mass action, the removal of retinal as well. Although the enhanced removal of retinol could also increase the rate constant for retinol formation, the similarity of the  $f_1$  values in the presence and absence of retinol elimination suggests that this is unlikely to be the case.

It is important to emphasize that the experiments presented in this work have measured the clearance of retinal; they have not directly measured the release and accumulation of retinal in living retina tissue and isolated cells. Such direct measurements are essential for understanding the handling of retinal by the cell and have been performed with isolated amphibian and lizard photoreceptors.<sup>60,61</sup> Unfortunately, the small size of the mouse photoreceptors presents technical challenges that are insurmountable at the present time.

To summarize, we have characterized the kinetics of retinol formation in the rod photoreceptors of mice lacking Abca4, rhodopsin kinase, arrestin, or the palmitate groups on rhodopsin. We found that retinol formation were not affected by the absence of any of these factors and appeared instead to depend on the kinetics of the reduction step. Retinal release from photoactivated rhodopsin in the absence of rhodopsin phosphorylation and arrestin binding is significantly faster than retinol formation. The activities of Abca4, rhodopsin kinase, and arrestin, would minimize the accumulation of retinal and protect against its toxicity.

### Acknowledgments

The authors thank Mas Kono for helpful discussions and Patrice Goletz for breeding the Palm<sup>-/-</sup> mice.

### References

- Ebrey T, Koutalos Y. Vertebrate photoreceptors. *Prog Retin Eye Res.* 2001;20:49–94.
- Palczewski K. G protein-coupled receptor rhodopsin. *Annu Rev Biochem.* 2006;75:743–767.
- Fain GL, Matthews HR, Cornwall MC, Koutalos Y. Adaptation in vertebrate photoreceptors. *Physiol Rev.* 2001;81:117–151.
- Burns ME, Arshavsky VY. Beyond counting photons: trials and trends in vertebrate visual transduction. *Neuron.* 2005;48:387–401.
- Saari JC. Biochemistry of visual pigment regeneration: the Friedenwald lecture. *Invest Ophthalmol Vis Sci.* 2000;41:337–348.
- Lamb TD, Pugh EN, Jr. Dark adaptation and the retinoid cycle of vision. *Prog Retin Eye Res.* 2004;23:307–380.
- Travis GH, Golczak M, Moise AR, Palczewski K. Diseases caused by defects in the visual cycle: retinoids as potential therapeutic agents. *Annu Rev Pharmacol Toxicol.* 2007;47:469–512.
- Palczewski K, Jager S, Buczylo J, et al. Rod outer segment retinol dehydrogenase: substrate specificity and role in phototransduction. *Biochemistry.* 1994;33:13741–13750.
- Futterman S, Hendrickson A, Bishop PE, Rollins MH, Vacano E. Metabolism of glucose and reduction of retinaldehyde in retinal photoreceptors. *J Neurochem.* 1970;17:149–156.
- Okajima TI, Pepperberg DR, Ripps H, Wiggert B, Chader GJ. Interphotoreceptor retinoid-binding protein: role in delivery of retinol to the pigment epithelium. *Exp Eye Res.* 1989;49:629–644.
- Qtaishat NM, Wiggert B, Pepperberg DR. Interphotoreceptor retinoid-binding protein (IRBP) promotes the release of all-trans retinol from the isolated retina following rhodopsin bleaching illumination. *Exp Eye Res.* 2005;81:455–463.
- Bernstein PS, Law WC, Rando RR. Isomerization of all-trans-retinoids to 11-cis-retinoids in vitro. *Proc Natl Acad Sci U S A.* 1987;84:1849–1853.
- Liu J, Itagaki Y, Ben-Shabat S, Nakanishi K, Sparrow JR. The biosynthesis of A2E, a fluorophore of aging retina, involves the formation of the precursor, A2-PE, in the photoreceptor outer segment membrane. *J Biol Chem.* 2000;275:29354–29360.
- Delmelle M. Retinal sensitized photodynamic damage to liposomes. *Photochem Photobiol.* 1978;28:357–360.
- Krasnovsky AA Jr, Kagan VE. Photosensitization and quenching of singlet oxygen by pigments and lipids of photoreceptor cells of the retina. *FEBS Lett.* 1979;108:152–154.
- Sommer ME, Smith WC, Farrens DL. Dynamics of arrestin-rhodopsin interactions: arrestin and retinal release are directly linked events. *J Biol Chem.* 2005;280:6861–6871.
- Hofmann KP, Pulvermuller A, Buczylo J, Van Hooser P, Palczewski K. The role of arrestin and retinoids in the regeneration pathway of rhodopsin. *J Biol Chem.* 1992;267:15701–15706.
- Sachs K, Maretzki D, Meyer CK, Hofmann KP. Diffusible ligand all-trans-retinal activates opsin via a palmitoylation-dependent mechanism. *J Biol Chem.* 2000;275:6189–6194.
- Weng J, Mata NL, Azarian SM, Tzekov RT, Birch DG, Travis GH. Insights into the function of Rim protein in photoreceptors and etiology of Stargardt's disease from the phenotype in abcr knockout mice. *Cell.* 1999;98:13–23.
- Sun H, Molday RS, Nathans J. Retinal stimulates ATP hydrolysis by purified and reconstituted ABCR, the photoreceptor-specific ATP-binding cassette transporter responsible for Stargardt disease. *J Biol Chem.* 1999;274:8269–8281.
- Beharry S, Zhong M, Molday RS. N-retinylidene-phosphatidylethanolamine is the preferred retinoid substrate for the photoreceptor-specific ABC transporter ABCA4 (ABCR). *J Biol Chem.* 2004;279:53972–53979.
- Stone EM, Webster AR, Vandenburgh K, et al. Allelic variation in ABCR associated with Stargardt disease but not age-related macular degeneration. *Nat Genet.* 1998;20:328–329.
- Allikmets R, Singh N, Sun H, et al. A photoreceptor cell-specific ATP-transporter gene (ABCR) is mutated in recessive Stargardt macular dystrophy. *Nat Genet.* 1997;15:236–246.
- Yamamoto S, Sippel KC, Berson EL, Dryja TP. Defects in the rhodopsin kinase gene in the Oguchi form of stationary night blindness. *Nat Genet.* 1997;15:175–178.
- Fuchs S, Nakazawa M, Maw M, Tamai M, Oguchi Y, Gal A. A homozygous 1-base pair deletion in the arrestin gene is a frequent cause of Oguchi disease in Japanese. *Nat Genet.* 1995;10:360–362.
- Chen CK, Burns ME, Spencer M, et al. Abnormal photoresponses and light-induced apoptosis in rods lacking rhodopsin kinase. *Proc Natl Acad Sci U S A.* 1999;96:3718–3722.
- Xu J, Dodd RL, Makino CL, Simon MI, Baylor DA, Chen J. Prolonged photoresponses in transgenic mouse rods lacking arrestin. *Nature.* 1997;389:505–509.
- Wang Z, Wen XH, Ablonczy Z, Crouch RK, Makino CL, Lem J. Enhanced shutoff of phototransduction in transgenic mice expressing palmitoylation-deficient rhodopsin. *J Biol Chem.* 2005;280:24293–24300.
- Chen C, Blakeley LR, Koutalos Y. Formation of all-trans retinol after visual pigment bleaching in mouse photoreceptors. *Invest Ophthalmol Vis Sci.* 2009;50:3589–3595.
- Fung BK, Hurley JB, Stryer L. Flow of information in the light-triggered cyclic nucleotide cascade of vision. *Proc Natl Acad Sci U S A.* 1981;78:152–156.
- Farrens DL, Khorana HG. Structure and function in rhodopsin: measurement of the rate of metarhodopsin II decay by fluorescence spectroscopy. *J Biol Chem.* 1995;270:5073–5076.
- Wu Q, Blakeley LR, Cornwall MC, Crouch RK, Wiggert BN, Koutalos Y. Interphotoreceptor retinoid-binding protein is the physio-

- logically relevant carrier that removes retinol from rod photoreceptor outer segments. *Biochemistry*. 2007;46:8669–8679.
33. Wenzel A, Reme CE, Williams TP, Hafezi F, Grimm C. The Rpe65 Leu450Met variation increases retinal resistance against light-induced degeneration by slowing rhodopsin regeneration. *J Neurosci*. 2001;21:53–58.
  34. Lyubarsky AL, Savchenko AB, Morocco SB, Daniele LL, Redmond TM, Pugh EN, Jr. Mole quantity of RPE65 and its productivity in the generation of 11-cis-retinal from retinyl esters in the living mouse eye. *Biochemistry*. 2005;44:9880–9888.
  35. Tsybovsky Y, Molday RS, Palczewski K. The ATP-binding cassette transporter ABCA4: structural and functional properties and role in retinal disease. *Adv Exp Med Biol* 703:105–125.
  36. Imai H, Kuwayama S, Onishi A, Morizumi T, Chisaka O, Shichida Y. Molecular properties of rod and cone visual pigments from purified chicken cone pigments to mouse rhodopsin in situ. *Photochem Photobiol Sci*. 2005;4:667–674.
  37. Chen J, Simon MI, Matthes MT, Yasumura D, LaVail MM. Increased susceptibility to light damage in an arrestin knockout mouse model of Oguchi disease (stationary night blindness). *Invest Ophthalmol Vis Sci*. 1999;40:2978–2982.
  38. Saari JC, Nawrot M, Kennedy BN, et al. Visual cycle impairment in cellular retinaldehyde binding protein (CRALBP) knockout mice results in delayed dark adaptation. *Neuron*. 2001;29:739–748.
  39. Lem J, Krasnoperova NV, Calvert PD, et al. Morphological, physiological, and biochemical changes in rhodopsin knockout mice. *Proc Natl Acad Sci U S A*. 1999;96:736–741.
  40. Matschinsky FM. Quantitative histochemistry of nicotinamide adenine nucleotides in retina of monkey and rabbit. *J Neurochem*. 1968;15:643–657.
  41. Mata NL, Weng J, Travis GH. Biosynthesis of a major lipofuscin fluorophore in mice and humans with ABCR-mediated retinal and macular degeneration. *Proc Natl Acad Sci U S A*. 2000;97:7154–7159.
  42. Wu Y, Fishkin NE, Pande A, Pande J, Sparrow JR. Novel lipofuscin bisretinoids prominent in human retina and in a model of recessive Stargardt disease. *J Biol Chem*. 2009;284:20155–20166.
  43. Kim SR, Jang YP, Jockusch S, Fishkin NE, Turro NJ, Sparrow JR. The all-trans-retinal dimer series of lipofuscin pigments in retinal pigment epithelial cells in a recessive Stargardt disease model. *Proc Natl Acad Sci U S A*. 2007;104:19273–19278.
  44. Jager S, Palczewski K, Hofmann KP. Opsin/all-trans-retinal complex activates transducin by different mechanisms than photolyzed rhodopsin. *Biochemistry*. 1996;35:2901–2908.
  45. Surya A, Knox BE. Enhancement of opsin activity by all-trans-retinal. *Exp Eye Res*. 1998;66:599–603.
  46. Tsina E, Chen C, Koutalos Y, et al. Physiological and microfluorometric studies of reduction and clearance of retinal in bleached rod photoreceptors. *J Gen Physiol*. 2004;124:429–443.
  47. Pawar AS, Qtaishat NM, Little DM, Pepperberg DR. Recovery of rod photoresponses in ABCR-deficient mice. *Invest Ophthalmol Vis Sci*. 2008;49:2743–2755.
  48. Philp NJ, Chang W, Long K. Light-stimulated protein movement in rod photoreceptor cells of the rat retina. *FEBS Lett*. 1987;225:127–132.
  49. Mangini NJ, Pepperberg DR. Immunolocalization of 48K in rod photoreceptors. Light and ATP increase OS labeling. *Invest Ophthalmol Vis Sci*. 1988;29:1221–1234.
  50. Whelan JP, McGinnis JF. Light-dependent subcellular movement of photoreceptor proteins. *J Neurosci Res*. 1988;20:263–270.
  51. Broekhuysse RM, Tolhuizen EF, Janssen AP, Winkens HJ. Light induced shift and binding of S-antigen in retinal rods. *Curr Eye Res*. 1985;4:613–618.
  52. Strissel KJ, Sokolov M, Trieu LH, Arshavsky VY. Arrestin translocation is induced at a critical threshold of visual signaling and is superstoichiometric to bleached rhodopsin. *J Neurosci*. 2006;26:1146–1153.
  53. Chen C, Koutalos Y. Rapid formation of all-trans retinol after bleaching in frog and mouse rod photoreceptor outer segments. *Photochem Photobiol Sci*.
  54. Heck M, Schadel SA, Marezki D, et al. Signaling states of rhodopsin. Formation of the storage form, metarhodopsin III, from active metarhodopsin II. *J Biol Chem*. 2003;278:3162–3169.
  55. Zimmermann K, Ritter E, Bartl FJ, Hofmann KP, Heck M. Interaction with transducin depletes metarhodopsin III: a regulated retinal storage in visual signal transduction? *J Biol Chem*. 2004;279:48112–48119.
  56. Park PS, Sapra KT, Jastrzebska B, et al. Modulation of molecular interactions and function by rhodopsin palmitoylation. *Biochemistry*. 2009;48:4294–4304.
  57. Maeda A, Maeda T, Golczak M, et al. Involvement of all-trans-retinal in acute light-induced retinopathy of mice. *J Biol Chem*. 2009;284:15173–15183.
  58. Hao W, Wenzel A, Obin MS, et al. Evidence for two apoptotic pathways in light-induced retinal degeneration. *Nat Genet*. 2002;32:254–260.
  59. Maeda A, Okano K, Park PS, et al. Palmitoylation stabilizes unliganded rod opsin. *Proc Natl Acad Sci U S A*. 107:8428–8433.
  60. Ala-Laurila P, Kolesnikov AV, Crouch RK, et al. Visual cycle: Dependence of retinol production and removal on photoproduct decay and cell morphology. *J Gen Physiol*. 2006;128:153–169.
  61. Kolesnikov AV, Ala-Laurila P, Shukolyukov SA, et al. Visual cycle and its metabolic support in gecko photoreceptors. *Vision Res*. 2007;47:363–374.